land

MDPI

Article

Holocene Vegetation Dynamics Revealed by a High-Resolution Pollen Record from Lake Yangzonghai in Central Yunnan, SW China

Min Wang [1], Qifa Sun [2], Hongwei Meng [1], Linpei Huang [1], Huayong Li [3], Hucai Zhang [4] and Caiming Shen [1,*]

[1] Yunnan Key Laboratory of Plateau Geographical Processes and Environmental Changes, Faculty of Geography, Yunnan Normal University, Kunming 650500, China; wang_min@ynnu.edu.cn (M.W.); menghw@ynnu.edu.cn (H.M.); linpei_huang@ynnu.edu.cn (L.H.)
[2] College of Resources, Environment and Chemistry, Chuxiong Normal University, Chuxiong 675000, China; sunqifa@cxtc.edu.cn
[3] School of Resource Environment and Tourism, Anyang Normal University, Anyang 455000, China; lhy@aynu.edu.cn
[4] Institute for Ecological Research and Pollution Control of Plateau Lakes, School of Ecology and Environmental Science, Yunnan University, Kunming 650500, China; zhanghc@ynu.edu.cn
* Correspondence: caiming_shen@ynnu.edu.cn

Abstract: Long-term regional vegetation dynamics is essential for the understanding of past land cover changes. High-resolution pollen analysis of a 1020 cm core from a large lake, Lake Yangzonghai (YZH), in central Yunnan, SW China, was conducted to reveal regional vegetation dynamics in the lake catchment over the past 13,400 years. Pollen record, principal component analysis (PCA) of pollen percentages of major arboreal taxa, and plant abundances estimated from the "Regional Estimates of VEgetation Abundance from Large Sites" (REVEALS) model show five successional stages of vegetation dynamics since 13,400 cal. a BP: regional vegetation with high coverages in the lateglacial (13,400–11,400 cal. a BP) was dominated by evergreen broadleaved forest (EBF) and deciduous broadleaved forest (DBF), together with some grass meadows and marshes; pine forest and alder forest expanded in the early Holocene (11,400–9000 cal. a BP) when vegetation coverages were still high; regional vegetation with low coverages was dominated by sweetgum forest, together with some pine forest during the mid-Holocene (9000–4200 cal. a BP); more pine forest, grass meadows and marshes occupied the lake catchment during the late Holocene (4200–800 cal. a BP), when vegetation coverages were higher than the average of the past 13,400 years; regional vegetation with low coverage was dominated by grass meadows and marshes, great deforestation happened in the last 800 years. Regional vegetation dynamics over the past 13,400 years in the Lake YZH catchment was the result of regional vegetation response to climate changes during the lateglacial and early–mid Holocene, and to human activities mainly during the late Holocene.

Keywords: fossil pollen; forest; vegetation coverage; Holocene; Yunnan

check for updates

Citation: Wang, M.; Sun, Q.; Meng, H.; Huang, L.; Li, H.; Zhang, H.; Shen, C. Holocene Vegetation Dynamics Revealed by a High-Resolution Pollen Record from Lake Yangzonghai in Central Yunnan, SW China. *Land* **2024**, *13*, 782. https://doi.org/10.3390/land13060782

Academic Editor: Le Yu

Received: 22 April 2024
Revised: 21 May 2024
Accepted: 29 May 2024
Published: 31 May 2024

Copyright: © 2024 by the authors. Licensee MDPI, Basel, Switzerland. This article is an open access article distributed under the terms and conditions of the Creative Commons Attribution (CC BY) license (https://creativecommons.org/licenses/by/4.0/).

1. Introduction

Vegetation is a fundamental component of terrestrial ecosystems [1]. Understanding how rapid climate change impacts these systems, especially the vegetative landscapes, is crucial amid escalating global warming and severe drought trends [2,3]. However, our understanding of past vegetation dynamics and land cover change in space and time falls far short of the requirements of climate and vegetation simulations for predicting future climate and vegetation change [4]. Lake sediments are natural archives of environmental changes [5]. Pollen analysis of lake sediments is an efficient method to reconstruct long-term vegetation dynamics and land cover changes [6,7].

The Holocene, directly preceding the Anthropocene, is a key period for understanding past vegetation dynamics and the interaction between vegetation and climate [8,9]. It

witnessed rapid warming after the Younger Dryas [10,11], and a series of centennial-scale cooling or drought events such as the 8.2 and 4.2 ka BP events [12–14], as well as a warm period with temperatures higher than today during the early–middle Holocene [8]. Therefore, Holocene vegetation dynamics is important for improving the predictability of future climate and vegetation.

Yunnan, located on the southeastern margin of the Tibetan Plateau, is the junction region of the South Asian and East Asian summer monsoon [15]. It is a pivotal region for investigating past vegetation dynamics within the context of the Asian monsoon system. So far, some studies on the reconstruction of Holocene vegetation in Yunnan [16,17] have been carried out. However, these studies used pollen data as proxies of climate changes rather than vegetation dynamics in response to climate change [18,19]. On the other hand, modern pollen processes such as pollen production rates and deposition are not considered completely in the interpretation of pollen percentage data [9,20].

Lake YZH, situated at the heart of Yunnan, is one of the nine largest lakes in Yunnan. It has uninterrupted Holocene sediments with a high deposition rate [21,22]. Our initial pollen analysis of coarse-resolution samples focused on Holocene climate change reflected by pollen data [21]. Here, we present a high-resolution pollen record from Lake YZH, and interrupt our pollen data with the aid of the REVEALS model to reveal the Holocene vegetation dynamics in response to monsoon climate changes in the catchment of Lake YZH, central Yunnan of SW China.

2. Location and Setting

Lake YZH (24°51′24″~24°57′58″ N, 102°58′47″~103°1′41″ E) is located at the junction of Chenggong and Yiliang in the east of Kunming, Southwest China (Figure 1a,b). It is a large and deep freshwater lake with an area of 31 km^2, an average water depth of 19.5 m, and a lake water level elevation of 1770 m a.s.l. Several streams (e.g., Yangzong, Shizhai, and Baiyi Rivers) flow into the lake, and its catchment area is about 192 km^2 [22]. Lake YZH does not have any natural outlet, but it has a man-made outlet, called the Tangchi Canal. This canal was excavated in 1388 AD to divert the lake water to irrigate the farmlands. The lake water now flows from this outlet on the lake's northeast side to the Nanpan River of the Pearl River System through the Yiliang Plain [23].

Topographically, about 6 km north of Lake YZH is the main peak of the Unna Mountains, Mount Laoye of 2730 m a.s.l. Its east and west banks are the extensions of the Unna Mountains. Mounts Xiangyang, Matou, Guanshan, Pingputou, Niujianbao, Gongshanding, and Doupuliangzi with elevations of 2523, 2242, 2156, 1991, 2281, and 2320 m a.s.l., respectively, appear from north to south within 5 km from the west lake shoreline. Mounts Yangjiaoshan, Liziji, Heilongshan, Heijiliangzi, Laotoushan, Laobaoshan, and Taipingshan with elevations of 2202, 2182, 2111, 2268, 2393, 2357, and 2397 m a.s.l., respectively, are located from north to south within 5 km from the east lake shoreline. Its south bank is occupied by the Yangzong Plain and lakeshore wetlands, and its north bank is occupied by the Tangchi Plain and lakeshore wetlands [23].

Climatologically, the catchment of Lake YZH has a subtropical monsoon climate over the low-latitude plateau, exhibiting obvious characteristics of wet and dry seasons (Figure 1c). Observational data of 1960–2019 at Yiliang meteorological station, the closest station to Lake YZH, show a mean annual temperature (MAT) of 16.6 °C, with the warmest temperature of 21.8 °C in June and the coldest temperature of 7.4 °C in January. The mean annual precipitation (MAP) is 890 mm, of which 765 mm (over 85%) is concentrated in the rainy season from May to October mostly brought about by the South Asian summer monsoon.

Phytogeographically, modern vegetation in the catchment of Lake YZH is dominated by two distinct vegetation types, i.e., pine forest and evergreen broadleaved forest (EBF). Pine forest consists mainly of *Pinus yunnanensis*, a widespread species in Yunnan with a broad ecological adaptability. EBF is dominated by *Cyclobalanopsis glaucoides*, *C. delavayi*, *Castanopsis delavayi*, and *C. orthocantha*, together with some species of *Quercus* and *Ilex*. Some

deciduous broadleaved species, including *Celtis yunnanensis*, *Pistacia chinensis*, *Crataegus scabrifolia*, *Albizia mollis*, *Broussonetia papyrifera*, *Alnus nepalensis*, *Platycarya strobilacea*, and *Quercus actuissima*, are mixed in EBF [24,25].

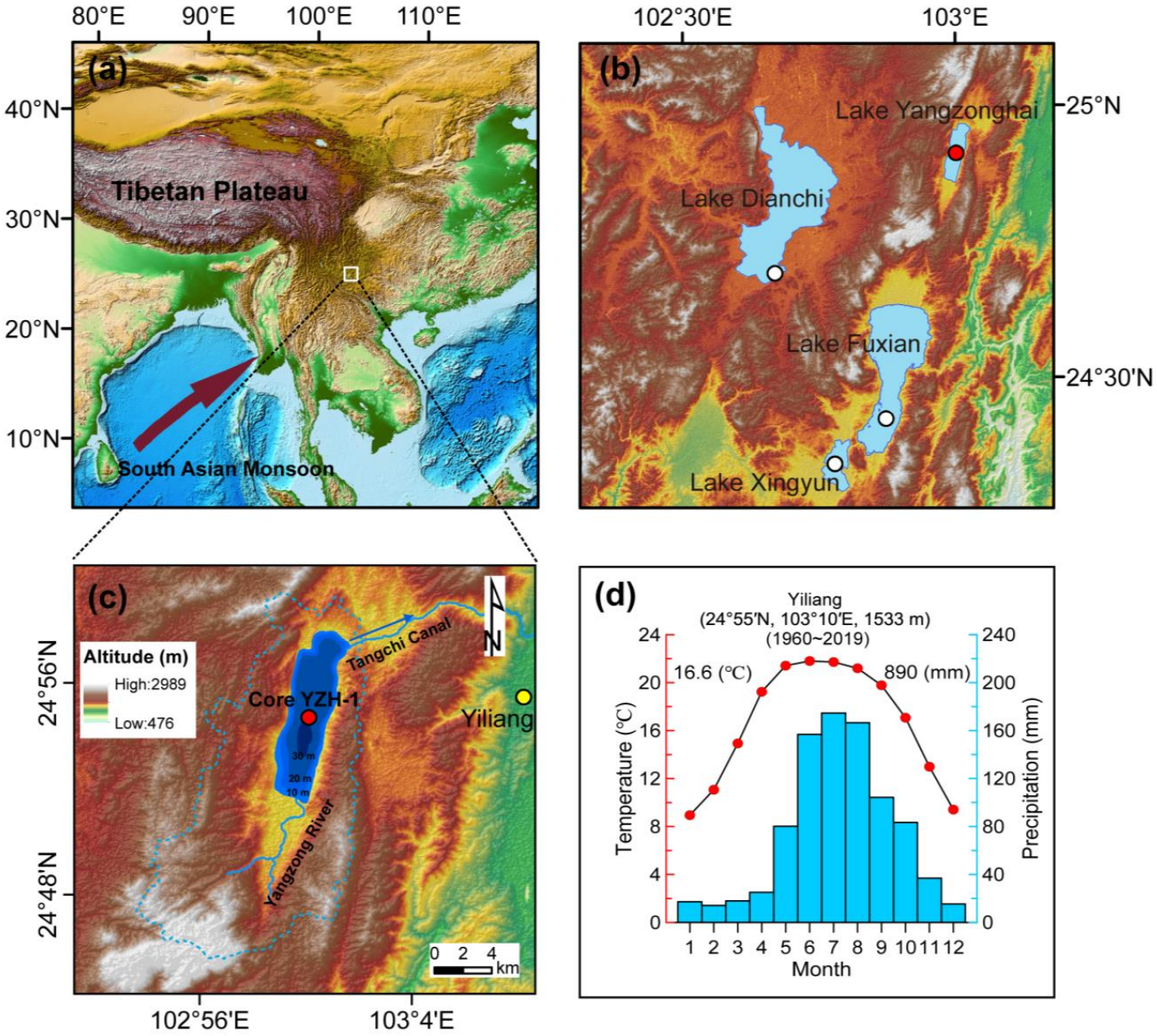


Figure 1. Topography, location, and climate of the study site, Lake YZH. (**a**) Topographic map showing the location of Lake YZH, in which the arrow displays the South Asian summer monsoon affecting the lake catchment; (**b**) topographic map showing the locations of Lakes YZH, Dianchi, Fuxian, Xingyun and their coring sites (red and white dots); (**c**) topographic map showing the Lake YZH catchment (blue dotted line), location of core YZH-1, and terrains around the lake; (**d**) monthly mean temperature and precipitation of 1960~2019 at Yiliang meteorological station near Lake YZH.

3. Materials and Methods

3.1. Lake Coring and Pollen Analysis

A 1020 cm sediment core (core YZH-1) was taken from the center of Lake YZH at a water depth of 23 m (Figure 1b) using the above-water platform and the Austrian UWITEC piston sampling equipment in July 2013. AMS ^{14}C dating of five leaf and two wood samples

was conducted at the Key Laboratory of Heavy Ion Physics, Ministry of Education, Peking University, China.

Core YZH-1 was sampled at 1 to 9 cm intervals for pollen analysis. In total, 185 pollen samples of 0.5–2 g were processed using the standard method involving HCl, KOH, HF, and acetolysis treatment [26]. Tablets containing a known quantity of *Lycopodium* spores were added as exotic markers into the samples to determine pollen concentrations and pollen influx values [27]. Pollen grains were identified and counted under the Olympus optical microscope (made by Olympus Corporation, Tokyo, Japan) with a magnification of 400 times. More than 500 pollen grains (830 grains for an average of 185 samples) were counted at each level. Pollen percentages were calculated on a sum of all terrestrial plant pollen. Pollen percentage and influx diagrams of selected pollen types were plotted using Tilia software version 3.0.1 [28]. Pollen zones of core YZH-1 were divided in terms of cluster analysis on the pollen percentage data of major pollen types [29].

Principal component analysis (PCA) of major arboreal pollen percentage data was employed to help the vegetational interpretation of pollen spectra and zones and to determine Holocene vegetation dynamics in the catchment of Lake YZH [30]. PCA was conducted in Canoco 5.

3.2. The REVEALS Model

We used the REVEALS model via the "disqover" package (version 0.9.09) [31] in R software (version 4.3.2) [32] to determine the relative pollen production (RPPs) across different plant taxa. The REVEAL model has been widely applied for the estimates of past regional plant abundance using fossil pollen records [9,33].

In order to run the REVEALS model, first, it is necessary to coordinate plant taxa with pollen types; plant/pollen taxa are then selected to estimate RPP. A reference taxon (RPP = 1) is used to calculate RPPs for all other taxa. Poaceae is often used as a common reference taxon because it is abundant in pollen and vegetation data [34]. In central Yunnan, we select Poaceae as a reference taxon as well. The REVEALS model requires an examination of the relative pollen productivity (RPPs) of various pollen taxa and the rate at which pollen falls in the study area. These parameters, along with fossil pollen counts, are used to adjust for the nonlinear relationship between a pollen taxon's percentage and its coverage area in the surrounding vegetation, ultimately to reconstruct the regional plant abundance of that taxon. A total of 15 pollen taxa RPPs are available in South China [35–38] (Table 1). We used these parameters to estimate Holocene plant abundance in the Lake YZH catchment.

Table 1. Relative pollen productivities (RPPs) with their standard errors (SEs) and fall speed of pollen (FSP) in South China.

Pollen Taxa	RPPs ± SE	FSP(m/s)	References
Tsuga	3.75 ± 0.5	0.056	[37]
Pinus	34.3 ± 3.09	0.041	[37]
Picea/Abies	2.55 ± 0.44	0.056	[36]
Deciduous *Quercus*	4.27 ± 0.04	0.025	[36]
Evergreen *Quercus*	5.19 ± 0.07	0.019	[36]
Castanopsis-type	10.67 ± 0.29	0.01	[37,38]
Ulmus	5.29 ± 0.8	0.027	[36]
Alnus	9.86 ± 0.09	0.021	[36]
Betula	10.26 ± 0.12	0.019	[36]
Pterocarya	8.07 ± 0.08	0.03	[35]
Liquidambar/Altingia	0.768 ± 0.029	0.036	[35]
Poaceae	1 ± 0.1	0.028	[36]
Artemisia	15.11 ± 0.37	0.012	[36]
Ranunculaceae	7.86 ± 2.65	0.01	[37]
Cyperaceae	4.17 ± 0.09	0.029	[36]

4. Results and Discussion

4.1. Stratigraphy and Chronology of Core YZH-1

The 1020 cm core sediments from Lake YZH consist predominantly of clayey silts. Three lithological units can be recognized from the sediment color (Figure 2). The sediment colors of 1020–392, 392–62, and 62–0 cm units are dark grey, light grey, and brick-red, respectively.

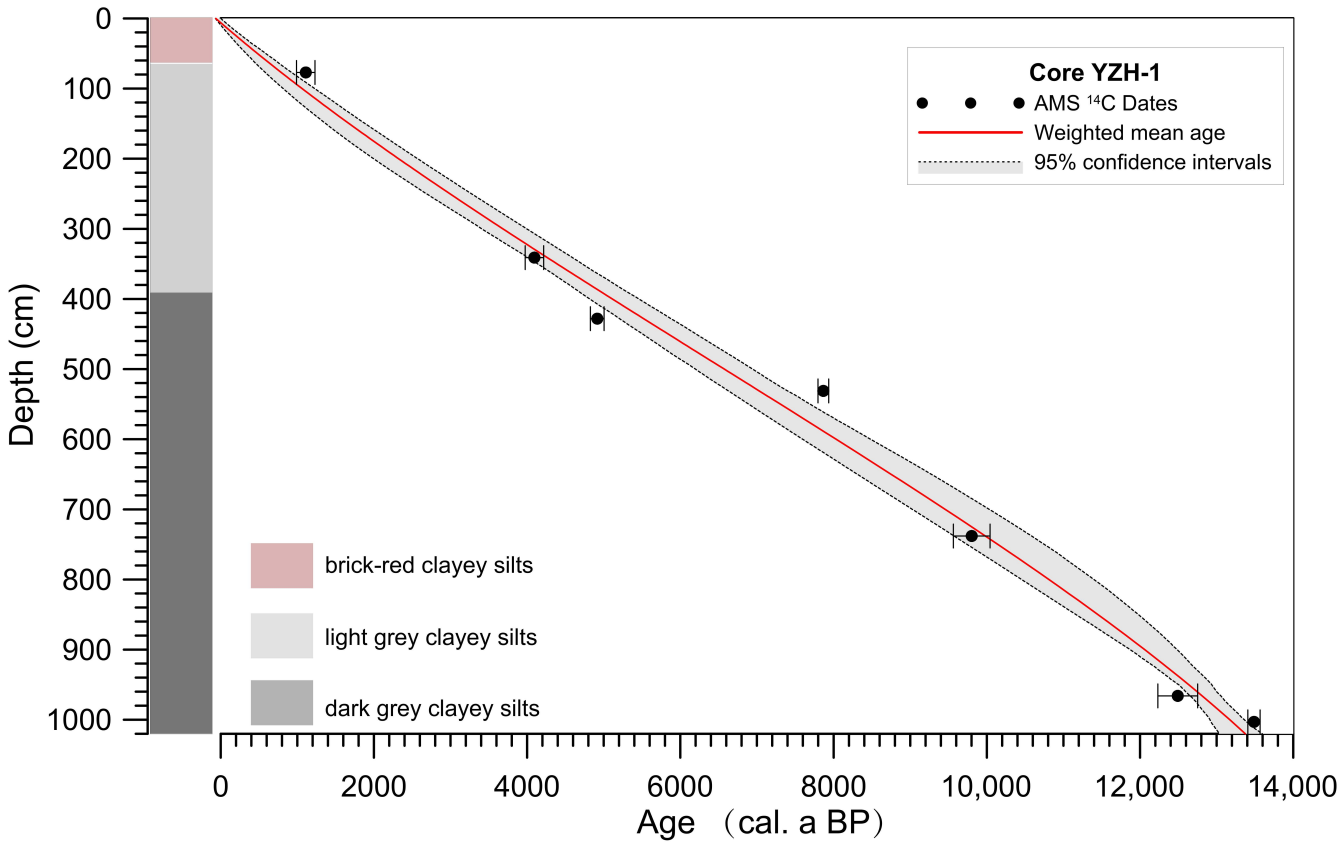


Figure 2. Lithology and age–depth model for core YZH-1 from Lake YZH.

This core is dated using seven reliable ^{14}C dates derived from leaves and wood (Table 2). These dates provide a good basis for the establishment of a reliable depth–age model. After the core top age was set as −63 cal. a BP, the final depth–age model (Figure 2) was established using a third power fitting of seven calibrated ages and the top age with the Clam package in R [39]. This model shows relatively high and continuous sedimentation rates, which vary between 0.68 and 0.99 mm/a. Low sedimentation rates less than 0.7 mm/a occur at the period of 8750–4520 cal. a BP, whereas high sedimentation rates more than 0.9 mm/a occur at the periods of 13,400–12,750 and 320 cal. a BP to the present.

Table 2. AMS ^{14}C dates of core YZH-1 from Lake YZH in central Yunnan, SW China.

Depth (cm)	^{14}C Dates (^{14}C a BP)	Calibrated Age * (cal. a BP)	Range § (cal. a BP)	Dating Material
77	1190 ± 30	1120	1005–1230	Leaves
341	3740 ± 30	4110	3985–4230	Leaves
428	4350 ± 30	4940	4850–5030	Wood
531	7030 ± 30	7870	7800–7940	Leaves
738	8790 ± 30	9900	9680–10,110	Leaves
966	10,470 ± 40	12,350	12,140–12,560	Wood
1003	11,550 ± 30	13,400	13,305–13,460	Leaves

* Calibrated using IntCal20 [40]; § Range of calibrated dates for mean ± 2σ.

4.2. Pollen Record from Lake YZH

Pollen spectra of core YZH-1 from Lake YZH are dominated by arboreal pollen (AP) (69–97.4%), mainly including pollen of coniferous, evergreen, and deciduous broadleaved taxa. Among coniferous taxa, *Pinus* is a dominant one, *Tsuga* is a common one, and *Picea/Abies*, *Podocarpus*, and *Dacrydium* are accidentally seen. Among evergreen and deciduous broadleaved taxa, evergreen *Quercus* [*Quercus* (E)] and *Castanopsis*-type (dominated by evergreen *Castanopsis* and *Lithocarpus* pollen, as well as few deciduous *Castanea* pollen) are mainly common evergreen taxa, deciduous *Quercus* [*Quercus* (D)], *Alnus*, *Ulmus*, *Betula*, *Pterocarya*, and *Liquidambar/Altingia* are common deciduous broadleaved taxa. Rosaceae is common evergreen and deciduous shrub taxa. The herbaceous pollen taxa contain mainly Poaceae, Ranunculaceae, *Artemisia*, Labiatae, and Cyperaceae. Pollen spectra of core YZH-1 are divided into five pollen zones in terms of the result of the CONISS analysis of pollen percentage data for major pollen taxa (their average percentages of all samples are more than 1%) (Figures 3 and 4):

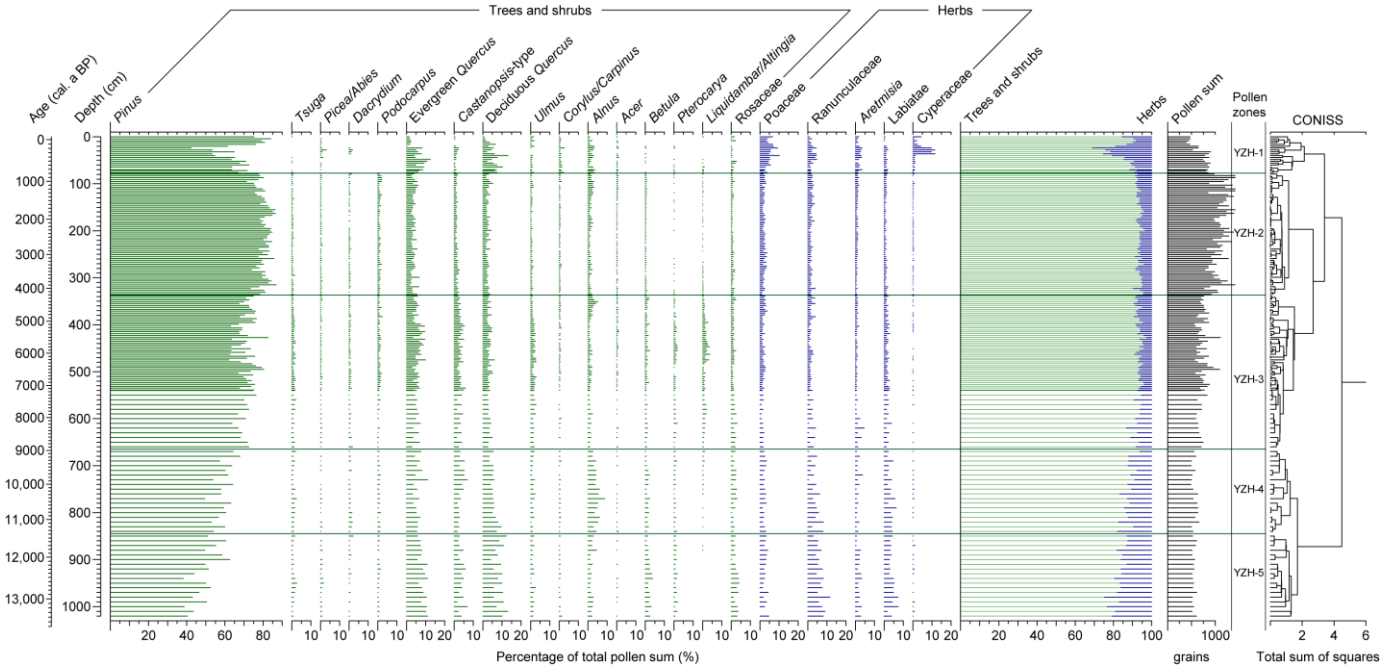


Figure 3. Pollen percentage diagram of major pollen taxa for core YZH-1 from Lake YZH.

Pollen zone YZH-5 (1020–845 cm; 13,400–11,400 cal. a BP): This basal pollen zone is characterized by the minimum of *Pinus*, maxima of *Quercus* (E) and *Quercus* (D), and of Ranunculaceae and Labiatae pollen for the entire pollen record. Pollen percentages of *Pinus*, *Quercus* (E), *Quercus* (D), Ranunculaceae, and Labiatae are 38.2–62.8/49.2% (minimum–maximum/average, the same as below), 5.6–11.1/8.6%, 4.1–13.0/8.6%, 2.9–11.6/6.5%, and 1.6–7.3/4.1%, respectively. Except for pollen taxa mentioned above, coniferous *Tsuga* and *Abies/Picea*, evergreen and deciduous broadleaved *Castanopsis*-type and shrub Rosaceae, as well as deciduous broadleaved *Ulmus*, *Alnus*, *Betula*, and *Pterocarya* are common. Among herbaceous pollen taxa, Poaceae and *Artemisia* are common, and Cyperaceae is occasionally present. Pollen influx values of this zone vary from 11,150 to 21,820 grains cm^{-2} a^{-1} with an average of 16,534 grains cm^{-2} a^{-1}, which is the second highest of the five pollen zones.

Pollen zone YZH-4 (845–665 cm; 11,400–9000 cal. a BP): This zone is marked by an increase in pollen percentages of *Pinus* (49.4–67.9/59.1%) and *Alnus* (2.2–8.8/4.4%). *Alnus* pollen reaches its maximum of the entire core. *Quercus* (E) (3.2–11.2/5.8%), *Quercus* (D) (3.2–9.6/5.6%), Rosaceae (0.2–3/1.6%), and Ranunculaceae (0.4–8.2/3.8%) pollen decreases. No significant changes occur in pollen percentages of *Castanopsis*-type, *Ulmus*, Poaceae, and Labitae. Pollen influx values in this zone exhibit a significant increase, reach-

ing 10,619–23,187/16,860 grains cm^{-2} a^{-1}, the pollen influx values slightly higher than zone YXH-5.

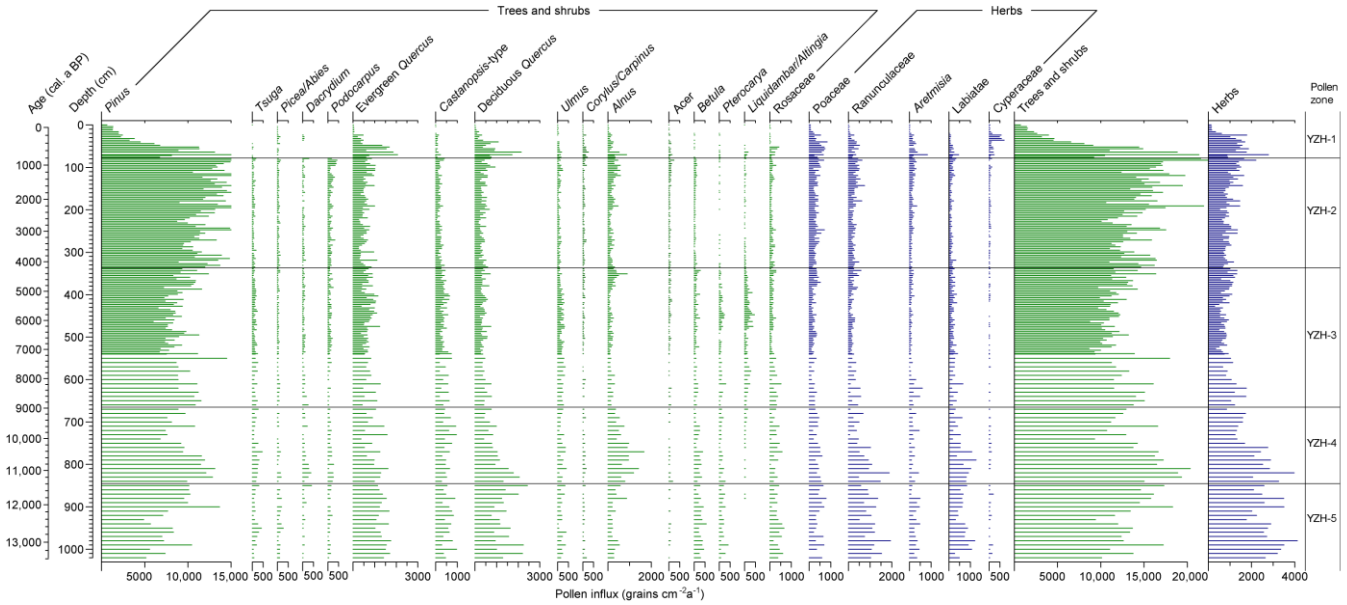


Figure 4. Pollen influx diagram of major pollen taxa for core YZH-1 from Lake YZH.

Pollen zone YZH-3 (665–337 cm; 9000–4200 cal. a BP): In this zone, *Pinus* pollen percentages (62–82.5/71.1%) continuously increase, and *Liquidambar/Altingia* pollen percentages (0–3.8/1.2%) increase to its maximum of the entire core. *Pterocarya* pollen decreases slightly, and *Acer* (0–1.2/0.3%) pollen increases slightly. *Quercus* (D) and *Alnus* pollen exhibit a nonlinear decline, and *Picea/Abies* pollen drops to its second minimum of the entire core. Herbaceous pollen percentages, especially Ranunculaceae and Labiatae, have a marked decrease. Pollen influx values of this zone show a high–low–high pattern. Pollen spectra at 665–533, 533–429, and 429–337 cm contain pollen influx values of 9897–19,013/14,147, 9004–14,038/11,514, and 10,526–17,689/13,071 grains cm^{-2} a^{-1}, respectively. Pollen zone YZH-2 (337–77 cm; 4200–800 cal. a BP): This zone is distinguished from zone YZH-3 by the maximum of *Pinus* pollen (71.3–86.8/80.3%) and significant decreases of *Quercus* (E) (1.7–6.6/3.7%), *Quercus* (D) (1.0–5.2/2.4%), *Castanopsis*-type (0.4–2.8/1.2%), and Rosaceae (0.1–1.8/0.7%). *Liquidambar/Altingia*, *Pterocarya*, and *Betula* pollen taxa occasionally appear at some levels. Pollen percentages of Poaceae, Ranunculaceae, Asteraceae, and *Artemisia* are as low as those in zone YZH-3. Pollen influx values (10,754–26,221/15,838 grains cm^{-2} a^{-1}) in this zone are as high as those of pollen spectra at the upper part (665–533 cm) of zone YZH-3, but they exhibit a marked zigzag.

Pollen zone YZH-1 (77–0 cm; 800 cal. a BP to the present): This zone is characterized by a significant nonlinear decrease of *Pinus* (42.4–84/66.5%), a continuous decline in pollen influx values, and an obvious increase in herbaceous pollen. *Quercus* (E) (0.2–12.5/5.6%), *Quercus* (D) (0.6–13.1/5.3%), *Corylus/Carpinus* (0.2–2.5/0.8%), Poaceae (2–10.1/5.1%), Ranunculaceae (0.4–4.8/2.3%), *Artemisia* (0–3.4/1.9%), and Cyperaceae (0.2–11.6/3.2%) pollen increase at the expense of *Pinus* pollen. *Liquidambar/Altingia*, *Pterocarya*, *Betula,* and *Tsuga* pollen taxa almost disappear in this zone. Pollen influx values exhibit a sharp downward trend, they vary from 840 to 24,137 grains cm^{-2} a^{-1} with an average of 8625 grains cm^{-2} a^{-1}, which is the lowest of the five pollen zones in core YZH-1.

4.3. Holocene Plant Abundance in the Lake YZH Catchment

The REVEALS was developed for pollen records from large lakes to estimate past plant abundance of regional vegetation composition (RVC) using fossil pollen counts [41], in which the regional plant abundance is expressed as the ratio of the pollen counts of each

taxon weighted by its pollen productivity and dispersal term to the total sum of those for all taxa [42,43]. In the catchment of Lake YZH, Poaceae was selected as a reference taxon, and 15 pollen taxa RPPs in South China (Table 1) were used to estimate their Holocene plant abundance via the "disqover" package. According to pollen zones of core YZH-1, its Holocene plant abundances of RVC (Figure 5) exhibit the following features:

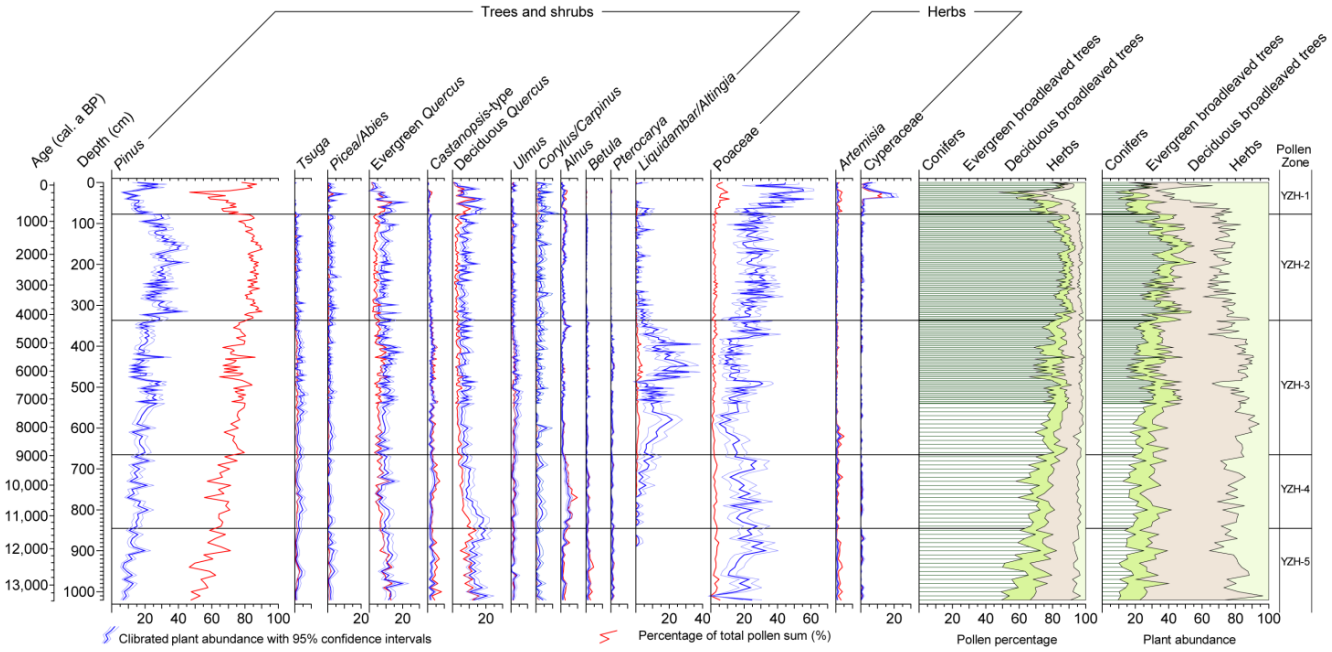


Figure 5. Diagram of plant abundances of major taxa estimated by REVEALS model in the Lake YZH catchment.

Pollen zone YZH-5 (1020–845 cm; 13,400–11,400 cal. a BP): Arboreal plants account for 64.3% (the zone average, the same as below), in which *Quercus* (D) (19%), *Quercus* (E) (15.5%), and *Pinus* (14.1%) are dominant trees, followed by *Castanopsis*-type (3.2%), *Betula* (1.7%), and *Alnus* (1.8%). Herbaceous plants (35.7%) are dominated by Poaceae, together with a few *Artemisia* (1.1%) and other taxa. The REVEALS-adjusted arboreal plant abundance is slightly lower than its pollen percentage; however, *Pinus* abundance is much less, and herbaceous plant abundance is much more than their pollen percentages.

Pollen zone YZH-4 (845–665 cm; 11,400–9000 cal. a BP): Arboreal plant abundance (67.3%) slightly increases, whereas herbaceous plant abundance (32.7%) slightly decreases. Arboreal plants are dominated by *Pinus* (19.4%), *Quercus* (D) (14.2%), and *Quercus* (E) (12%); *Alnus* (4.9%) and *Castanopsis*-type (3.4%) are common. Herbaceous plants are dominated by Poaceae (25.1%).

Pollen zone YZH-3 (665–337 cm; 9000–4200 cal. a BP): Arboreal plant abundance reaches its maximum (76.7%) of the entire core. Among arboreal plants, *Liquidambar/Altingia* and *Ulmus* also reach their maxima (16.7% and 3.4%), and other abundant taxa include *Pinus* (24.7%), *Quercus* (E) (12.2%), and *Quercus* (D) (8.3%), *Castanopsis*-type (3.1%), *Alnus* (1.5%), and *Tsuga* (3.4%). Herbaceous plants (23.3%) are dominated by Poaceae (19.7%). At the depth of 493–485 cm (6510–6390 cal. a BP), there is a significant decrease in abundances of *Liquidambar/Altingia* (3.4%) and *Quercus* (E) (9.9%), and a significant increase in Poaceae abundance (32.7%).

Pollen zone YZH-2 (337–77 cm; 4200–800 cal. a BP): Arboreal plant abundance falls to 64.9%, the third lowest level of the entire core. Among arboreal plants, *Pinus* abundance increases to 35.3%, whereas abundances of evergreen broadleaved taxa such as *Quercus* (E) (10%) and *Castanopsis*-type (1.7%) as well as deciduous broadleaved taxa such as *Quercus* (D) (8.2%), *Liquidambar/Altingia* (1.9%), and *Ulmus* (1.5%) decrease. Herbaceous plants (35.1%) are still dominated by Poaceae (29.9%).

Pollen zone YZH-1 (77–0 cm; 800 cal. a BP to the present): Arboreal plant abundance falls further to the minimum (46.2%) of the entire core. Among arboreal plants, *Quercus* (D) (10.7%) increases, whereas other arboreal taxa such as *Pinus* (18.7%), *Quercus* (E) (9.6%), *Castanopsis*-type (0.5%), and *Ulmus* (1.3%) decrease; some taxa such as *Liquidambar/Altingia*, *Betula*, and *Pterocarya* tend to disappear. Herbaceous plant abundance reaches its maximum (53.8%) of the entire core; significant increases in plant abundances are Poaceae (43.8%) and Cyperaceae (6.1%); other herbs such as *Artemisia* (1%) are common.

Plant abundances above in the Lake YZH catchment were estimated from the REVEALS model. However, it should be pointed out that Lake YZH is a large one with an area of more than 30 km^2 inflowed by several rivers, and its shape is rectangular. The main assumptions of the REVEALS model, e.g., the wind is the major agent of pollen transport and the lake shape is circular [41,43], are not satisfied completely for Lake YZH. Furthermore, RPPs of pollen taxa (Table 1) used in this study just cover the major part of fossil pollen taxa from Lake YZH. Therefore, plant abundances estimated from the REVEALS model in the Lake YZH catchment could have certain uncertainties.

4.4. Holocene Forest Types in the Lake YZH Catchment

To reveal Holocene forest types growing in the Lake YZH catchment, PCA of fossil arboreal pollen data was employed. This dataset consists of 185 samples (levels) and 16 arboreal pollen taxa, i.e., *Pinus*, *Tsuga*, *Picea/Abies*, *Podocarpus*, *Dacrydium*, *Quercus* (E), *Castanopsis*-type, *Quercus* (D), *Acer*, *Alnus*, *Ulmus*, *Betula*, *Corylus/Carpinus*, *Pterocarya*, *Liquidambar/Altingia*, and Rosaceae. The result of PCA shows that the first two principal components explain 33.8% and 13.6% variations of the dataset.

In the biplot of the first two principal component axes (Figure 6), the ordination of samples is directly related to the ordination of pollen taxa, i.e., samples having high scores on an axis are dominated by pollen types having high scores on that axis [44]. The first principal component axis separates the pine forest on the negative end from all other forest types. Typical pine forest is represented by fossil pollen spectra of pollen zone YZH-2. On the positive end is EBF dominated by *Quercus* (E), *Castanopsis*-type, Rosaceae, *Quercus* (D), *Pterocarya*, and *Betula*. EBF is represented by fossil pollen spectra of pollen zones of both YZH-4 and YZH-5. The discrete distribution of those fossil pollen samples in the biplot of PCA implies the occurrence of several EBF types with different dominant and constructive elements. The second principal component axis separates *Liquidambar/Altingia* forest (probably sweetgum forest) on the positive end and other deciduous broadleaved forests (DBFs). Sweetgum forest is represented by fossil pollen spectra of pollen zone YZH-3, and fossil pollen spectra of pollen zones YZH-1, YZH-4, and YZH-5 contain DBFs. The centers of pollen zones YZH-1 to 5 show a vegetation successional trajectory of the entire fossil pollen sequence.

Hemlock forest is dominated by *Tsuga dumosa*, together with some *Quercus pannosa*, *Rhododendron yunnanense* and *Abies georgei*. It occurs in northwestern Yunnan to the west and north of the Wuliangshan mountains. Hemlock, growing in mountains of 2300–3200 m a.s.l., is a cool-temperate tree species favoring MAT of 6–12 °C, MAP of more than 700 mm, and relative humidity of larger than 75%. Cold-temperate fir/spruce forests grow in subalpine mountains of 3000–4000 m a.s.l. Hemlock and fir/spruce forests reflected by pollen spectra just occur in small areas on mount peaks around Lake YZH.

EBF is widely distributed in Yunnan. Ecologically, it contains warm EBFs in central and northern Yunnan and warm–hot EBFs in southern Yunnan. Warm EBFs include a series of types due to the diversity of constructive and dominant species. *Lithocarpus craibianas*, *L. variolosus*, and *L. cleistocarpus-Castanopsis platyacantha* forests are common in northwestern, central, and northeastern Yunnan, respectively. *Cyclolanbanopsis glaucoides*, and *C. delavayi* forests occur in mountains below 2100 m a.s.l., central Yunnan. *Castanopsis delavayi* forests are found in Yunnan, whereas *C. orthacantha* forests are distributed in mountains of 1900–2600 m a.s.l., central Yunnan. Warm–hot EBFs include *Castanopsis hystrix-C. indica*, *C. fleuryi-Lithocarpus truncates*, and *C. fabri-C. calathiformis* forests [44].

EBFs indicated by pollen spectra of different pollen zones thus reflect different EBFs under different climatic conditions.

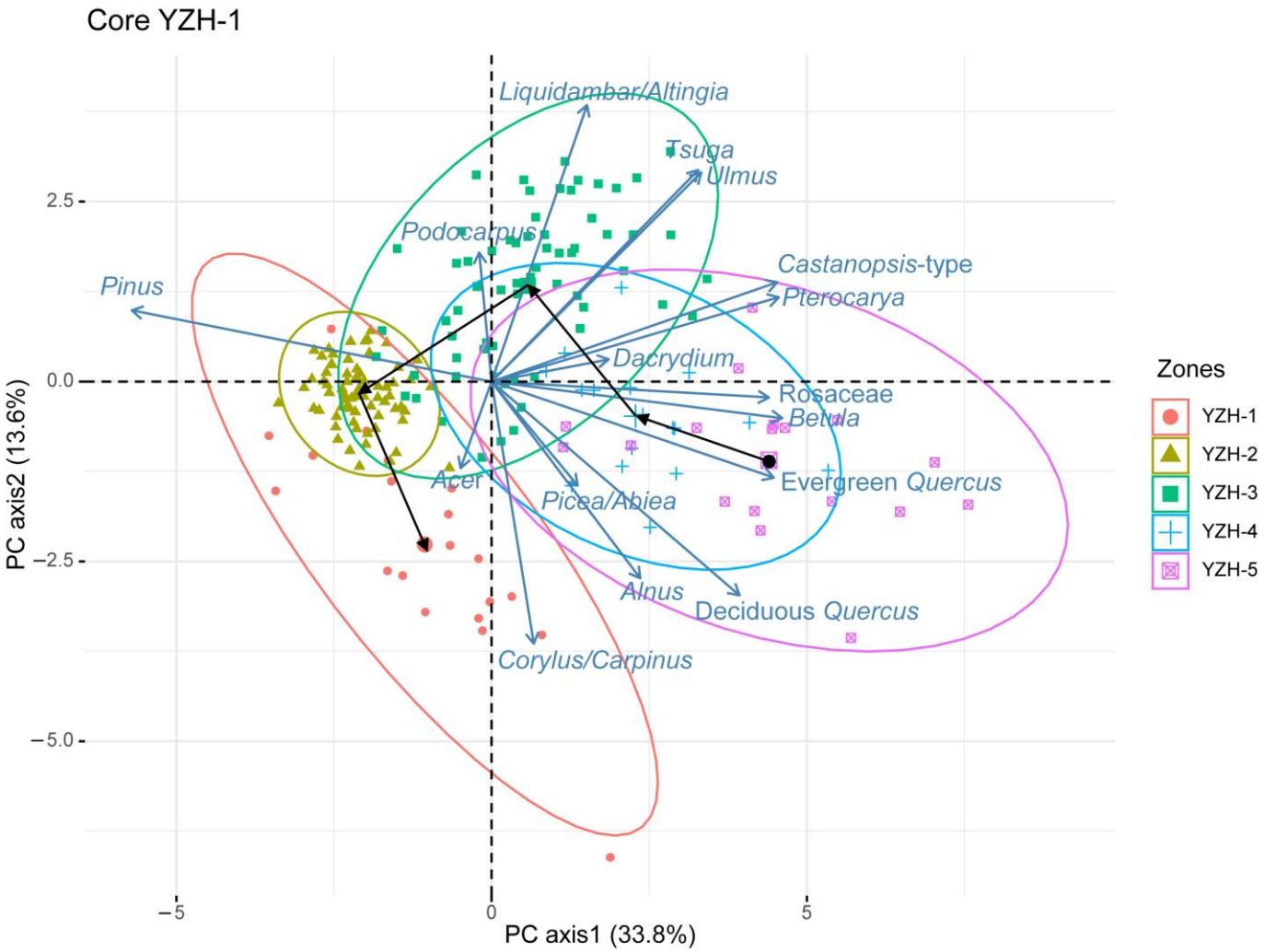


Figure 6. Biplot of PCA on pollen percentages of sixteen arboreal pollen taxa for core YZH-1 from Lake YZH. The samples were grouped in terms of pollen zones. The arrows show the trajectory of pollen zone centers.

In Yunnan, especially central Yunnan, pine forests are dominated by *Pinus yunnanensis* [45]. *Pinus yunnanensis* forest occurs over a great altitudinal range between extremes of 600 and 3500 m a.s.l. Its climatic preference is for small seasonal temperature differences, wet summer and autumn, and dry winter and spring. It contains several subtypes, such as *P. yunnanensis-Quercus pannosa*, *P. yunnanensis-P. armandii*, *P. yunnanensis*-shrubs, *P. yunnanensis*-grasses, *P. yunnanensis-Alnus nepalensis*, *P. yunnanensis-Cyclobalanopsis delaviya*, *P. yunnanensis-Keteleeria eyelyniana*, *P. yunnanensis-Quercus acutissima-Q. variabilis*, *P. yunnanensis-Q. franchetii*, and *P. yunnanensis-Schima wallichii* forests [44]. Therefore, *Pinus yunnanensis* forests indicated by pollen spectra of different pollen zones may reflect its different subtypes.

DBF is also widely distributed in Yunnan. Ecologically, it includes cold-temperate, cool-temperate, warm, and warm–hot DBFs. Cold-temperate DBFs, such as *Quercus pannosa*, *Q. aguifolioides*, *Betula abo-sinensis,* and *B. platyphylla* forests, are found in northwestern Yunnan. Cool-temperate DBF such as *Acer* spp. forest grows in northwestern Yunnan too, whereas another one, *Quercus dentata* forest, grows in mountains of 1900–2800 m a.s.l. of northwestern, central, and southeastern Yunnan. Warm DBFs contain *Alnus nepalensis*,

Quercus acutissima, *Q. variabilis*, *Q. aliena* var. *acuteserrata*, *Juglans sigillata*, and *Castanea mollissima* forests, which mainly occur in central and northern Yunnan. *Betula alnoides* forest and *Liquidambar formosana* forest are two major warm–hot DBFs. *Betula alnoides* forest grows in southern Yunnan, while *Liquidambar formosana* forest grows in southeastern Yunnan [45]. DBFs indicated by pollen spectra of different pollen zones may include oak, alder, and birch forests.

4.5. Holocene Regional Vegetation Dynamics in the Lake YZH Catchment

As shown in Figures 3–7, Holocene regional vegetation dynamics in the Lake YZH experienced five successional stages:

Stage 5 (13,400–11,400 cal. a BP; pollen zone YZH-5): In the Lake YZH catchment, its lakeside wetlands were occupied presumably by grass meadows and marshes, its lowlands and hilly terrains by EBFs, DBFs, and pine forests, and peaks of mounts around the lake by few montane cool-temperate hemlock forests and cold-temperate fir/spruce forests. EBFs of ca. 18% of RVC are dominated by *Lithocarpus*, *Castanopsis*, *Cyclobalanopsis*, and evergreen *Quercus*, together with some deciduous broadleaved trees and shrubs. DBFs of ca. 26% of RVC are dominated by deciduous oaks, elms, alders, birches, and wingnuts. Pine forest of ca. 14% of RVC is likely dominated by *Pinus yunnanensis*, together with, probably, a few *P. armandii*. Grass meadows and marshes of ca. 35% of RVC are dominated by Poaceae, Labitae, Raununculaceae, and Cyperaceae herbs. Meanwhile, Pollen influx, a proxy of vegetation coverage [46], shows dense vegetation in the lake catchment; however, the vegetation coverage of this stage experienced high–low–high three successional substages. A marked drop in vegetation coverage around 12,300 cal. a BP suggests the occurrence of an abrupt centennial vegetation shift event.

Stage 4 (11,400–9000 cal. a BP; pollen zone YZH-4): Forests occupying the lake catchment were still those occurring in the previous stage. However, pine and alder forests expanded significantly to ca. 19% and 5% of RVC at the expense of EBFs (ca. 15% of RVC) and other DBFs. Among DBFs, sweetgum forests began to appear and gradually formed a certain scale (ca. 9% of RVC). The peaks of mounts near the lake are still occupied by hemlock and fir/spruce forests, but more hemlock forests and less fir/spruce forests. Grass meadows and marshes of ca. 33% of RVC occupied the lakeside wetlands. Vegetation coverages reached their maximum of the past 13,400 years at 11,400–10,000 cal. a BP, and then dropped to lower than the average of the entire sequence at 10,000–9000 cal. a BP.

Stage 3 (9000–4200 cal. a BP; pollen zone YZH-3): Pine forest (ca. 25% of RVC) continued to expand, and EBFs maintained as much as the previous stage. Sweetgum forest reached its maximum (ca. 17% of RVC) in this stage, but its abundance exhibited a fluctuation of rise–drop–rise–drop. Sweetgum forest gradually rose from ca. 8 to 28% of RVC at 9000–7500 cal. a BP, and dropped nonlinearly to zero at 7500–6350 cal. a BP, then rose again to 38% of RVC at 6350–5000 cal. a BP, finally declined nonlinearly to 4% of RVC at 5000–4200 cal. a BP. Hemlock and fir/spruce forests were as much as those in the previous stage, and grass meadows and marshes (ca. 23% of RVC) decreased significantly. Vegetation coverages of this stage were the second lowest among five stages over the past 13,400 years, with a period of vegetation coverages slightly higher than the average of the entire sequence at 9000–7100 cal. a BP and a period of vegetation coverages lower than the average of the sequence at 7100–4200 cal. a BP. It should be pointed out that an abrupt centennial vegetation shift occurred at 6600–6350 cal. a BP. This shift is characterized by a marked decrease in sweetgum forests, an obvious increase in pine forests, grass meadows, and marshes, as well as a significant drop in vegetation coverage.

Stage 2 (4200–800 cal. a BP; pollen zone YZH-2): Pine forest (ca. 35% of RVC) expanded further to reach its maximum, whereas DBFs (ca. 14% of RVC) thinned to their minima. Among DBFs, sweetgum forests gradually decreased to nearly disappear. EBFs slightly decreased, and hemlock and fir/spruce forests almost disappeared in regional vegetation. Grass meadows and marshes (ca. 35% of RVC) increased significantly. Vegetation coverages

kept a level close to the average of the entire sequence from 4200 to 2550 cal. a BP, and then increased to the second highest level of the entire sequence from 2550 to 800 cal. a BP.

Stage 1 (800 cal. a BP to the present; pollen zone YZH-1): After 800 cal. a BP, the pine forest shrank rapidly to its minimum around 200 cal. a BP, and then it expanded to the level at the average of the entire sequence. DBFs and EBFs exhibited nonlinear decrease trends until now, whereas grass meadows and marshes (ca. 53.8% of RVC) showed an opposite pattern to pine forests, i.e., expanding to their maxima, and then shrinking. Vegetation coverages at this stage exhibited a continuing downward trend, and reached its minimum recently. At 400–160 cal. a BP occurred the third abrupt centennial vegetation change event, characterized by a drop in plant abundances of pine and deciduous broadleaved trees, as well as a rise in plant abundances of herbs.

Overall, regional vegetation dynamics over the last 13,400 years in the lake catchment experienced five stages. Stage 5 saw regional vegetation dominated by EBFs and DBFs, as well as some grass meadows and marshes; and stage 4 witnessed expansion of pine and alder forests. Regional vegetation was dominated by sweetgum and pine forests in stage 3, and more pine forests, grass meadows, and marshes occurred in the lake catchment in stage 2. In stage 1, regional vegetation was dominated by grass meadows and marshes, and great deforestation happened.

4.6. Holocene Regional Vegetation Dynamics in Response to Climate Change and Human Activities in the Lake YZH Catchment

Pollen record from Lake YZH reveals five stages (equivalent to five pollen zones) with relatively stable regional vegetation, four major vegetation transitions (equivalent to four boundaries of five pollen zones), and three possible centennial vegetation shift events (Figure 7). Pollen records from other large lakes in central Yunnan such as Lakes Dianchi [47], Fuxian [48], and Xingyun [49] (Figure 8) show similar patterns of vegetation change, supporting our results, although some differences occur among these pollen records due to possible differences in landscapes and vegetation types in the lake catchments, as well as dating uncertainties, sedimentary rate, sampling resolution, and determining criteria of pollen zones of these pollen records. Furthermore, a comparison of vegetational dynamics in the Lake YZH catchment with regional hydrothermal conditions [50–52], forest fires (Figure 7), and human activities [53,54] suggests that the major vegetation changes were the result of regional vegetation responses to climate changes and human activities.

Chronologically, stage 5 at 13,400–11,400 cal. a BP is approximately equivalent to the Younger Dryas Chron of the lateglacial. A Holocene mean annual air temperature (MAAT) record reconstructed from branched glycerol dialkyl glycerol tetraethers (brGDGTs) of the same core used in this study from Lake YZH shows regional temperatures of ca. 3 °C lower than the present, and an oxygen isotope record of stalagmites at Dongge Cave, a proxy of Asian summer monsoon strength [51], indicates a weak summer monsoon in this stage. Regional vegetation of the Lake YZH catchment involves fewer EBFs, more DBFs, few montane hemlock and fir/spruce forests, and some grass meadows and marshes. Similar regional vegetation was also found in the catchments of other lakes [47–49] (Figure 8), except more pine forest in the Lake Dianchi catchment, and more deciduous oak forest and fir/spruce forest in the Lake Xingyun catchment. No montane hemlock and fir/spruce forests grow now in the four lake catchments, implying colder and relatively drier than the present climatic conditions in this stage, as indicated by the brGDGTs-based temperature record and stalagmite oxygen isotope record. A possible abrupt centennial vegetation thinning event occurred following the low temperature and the weakest Asian summer monsoon around 12,300 cal. a BP; the highest forest fire frequency over the past 13,400 years occurred during this stage in the Lake YZH catchment, which was likely related to weakening monsoon and more deciduous forests.

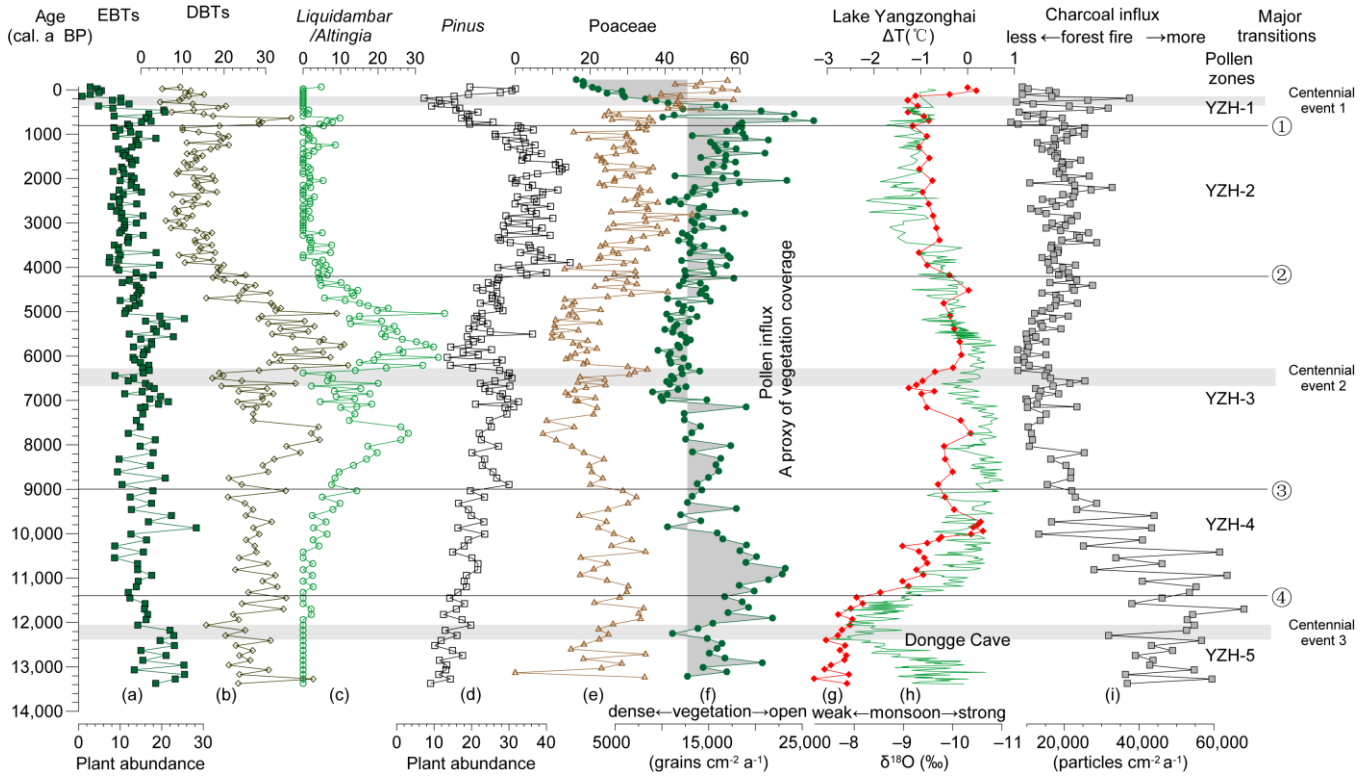


Figure 7. A comparison of the plant abundances of different vegetation types, including EBFs (**a**), DBFs (**b**), sweetgum forests (**c**), pine forests (**d**), and grass meadowa and marshes (**e**), with vegetation coverage (**f**), brGDGTs-based temperature record from Lake YZH (**g**) [50], stalagmite oxygen isotope record from Dongge Cave (**h**) [52], and charcoal influx (a proxy of forest fire) from Lake YZH (this study) (**i**).

The Younger Dryas Chron was followed by the early Holocene of warming and Asian summer monsoon strengthening [50,51,55]. Regional vegetation in the Lake YZH catchment experienced a major vegetation transition from stages 5 to 4 around 11,400 cal. a BP. After this transition, pine and alder forests expanded in the Lake YZH catchment, while EBFs, elm, and sweetgum forests increased in the catchments of other lakes. Subtropical deciduous alder forest grows on slopes and in lower parts of valleys, 1800–3150 m a.s.l., commonly as secondary vegetation types [56]. Elm forests in Yunnan include *Ulmus tonkinensis* in southeast Yunnan, *U. lanceaefolia* in southwest Yunnan, and *U. kunmingensis* in central Yunnan; the former two species are main components of warm–hot broadleaved forest, and the latter species is a common element of the warm broadleaved forest [57]. Sweetgum forest is a major warm–hot DBF. It is evident that the appearance and expansion of these forests were the results of regional vegetation in response to the amelioration of climatic conditions. Forest fires gradually became less, probably due to the increase of monsoonal rainfall.

The Lake YZH catchment witnessed another major vegetation transition from regional vegetation stages 4 to 3 around 9000 cal. a BP. In stage 3, sweetgum forest expanded to its maximum in the past 13,400 years. As a warm–hot southern subtropical DBF, sweetgum forest, favoring wet and hot climatic conditions, grows in hilly terrains where MAT is 16–20 °C with extreme warmest temperature of ca. 36 °C, and MAP is 900–1200 mm. The maximal sweetgum forests also occurred in the lake catchments of central Yunnan. This fact suggests the occurrence of the Holocene climate optimum (HCO) with the maximum temperature and summer monsoon intensity at 9000–4200 cal. a BP in central Yunnan. The HCO existed commonly in records of climate proxies and climate reconstructions in the South Asian monsoon domain [55,58]. An abrupt centennial vegetation shift occurred at 6600–6350 cal. a BP in the Lake YZH catchment, which probably is the result of regional

vegetation response to possible cooling and monsoon weakening events [50,59]. Although this event does not get as much attention as those Holocene Bond events [60], it also left hints in the oxygen isotope record of stalagmites at Dongge Cave [51] (Figure 8). This stage witnessed the least forest fires, presumably because of high monsoonal rainfall.

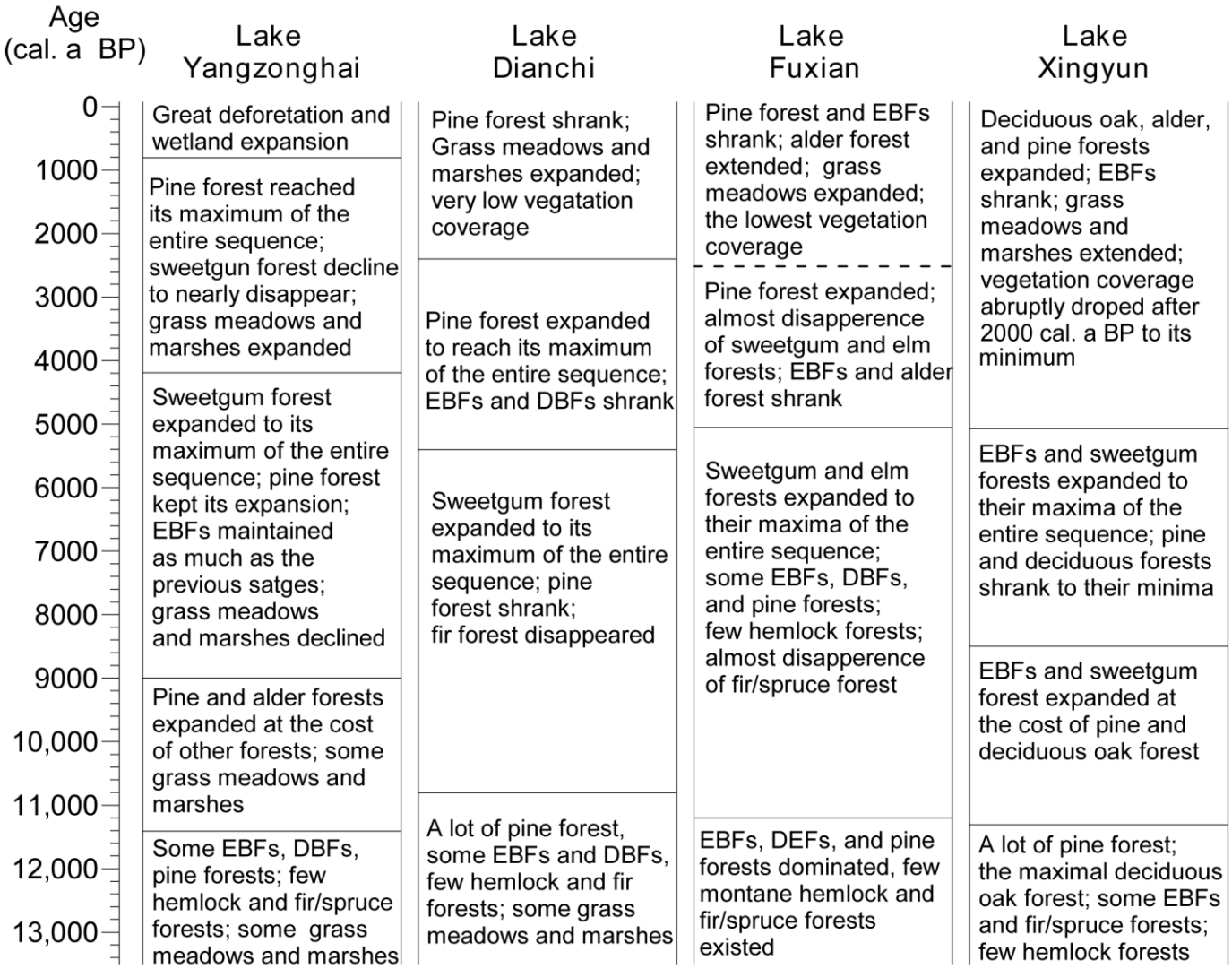


Figure 8. A comparison of regional vegetation dynamics in the catchments of Lakes YZH, Dianchi, Fuxian, and Xingyun. Dotted line displays pollen subzone boundary.

After 4200 cal. a BP, regional vegetation changed from sweetgum forest-dominated to pine forest-dominated in the Lake YZH catchment as well as in other lake catchments of central Yunnan, following temperature cooling and monsoon weakening. However, pollen influx, as a proxy of vegetation coverage, exhibited an increasing trend and plant abundances of pine—a decreasing trend after 2000 cal. a BP. This phenomenon can be interpreted by the deforestation of pine forests increasing erosion intensity, which results in a high sedimentary rate, and thus high pollen influx values [61]. This interpretation is supported by archaeological evidence and historical documents. The bronze culture reached its highest level and began the transition to the Iron Age in the Dianchi area at about 2200 BP (before the present) when much of the coals needed for bronze and/or iron smelting would come from cutting down large numbers of trees [62], as partially indicated by an increase of charcoal influx (more forest fires). Tien became a vassal kingdom of Han China at 2090 BP. Wen Chi, the Han governor of the Dianchi area, introduced terraced and irrigated fields at about 1780 BP for the first time. The Nan Zhao people in the Lake

Erhai catchment increasingly migrated into the Dianchi area from 1290 BP, and a city (Tue Dong) was established close to the northern end of Lake Dianchi by 1230 BP. In total, 10,000 additional families from north China were brought to the Dianchi area thirty years later, when rice was grown in the valleys and wheat on the terraced slopes, and streams were used for irrigation [63]. As the population grew and agriculture developed, the demands for land became greater and greater, and deforestation and the expansion of arable land were thus inevitable.

In those lake catchments of central Yunnan, deforestation continued as well as grass meadows and marshes expanded after 800 cal. a BP, and forests recently reached their minima. During this stage, especially the Ming and Qing dynasties, mass migration into Yunnan happened, and a large of garrison troops and peasants were arranged in the lake catchment to make land reclamation further expand, and thus great deforestation [62]. The third abrupt centennial vegetation change event at 400–160 cal. a BP was mainly attributed to human activities, partially to a possible Little Ice Age cooling event.

5. Conclusions

A high-resolution pollen analysis of a 1020 cm core from Lake YZH was conducted in this study to reveal regional vegetation dynamics in the lake catchment over the past 13,400 years. We obtained the following conclusions:

1. Regional vegetation over the past 13,400 years in the Lake YZH catchment experienced five successional stages and four major transitions. The Younger Dryas Chron (13,400–11,400 cal. a BP) witnessed various vegetation types, including EBFs, DBFs, pine forests, hemlock forests, fir/spruce forests, grass meadows, and marshes. The early Holocene (11,400–9000 cal. a BP) saw significant expansions of pine, alder, and sweetgum forests. The mid-Holocene (9000–4200 cal. a BP) witnessed a great expansion of sweetgum forest to its maximum of the past 13,400 years. Pine forest expanded to its maximum, and sweetgum forest shrank to nearly disappear during the late Holocene (4200–800 cal. a BP). The last 800 years saw great deforestation and a big expansion of grass meadows and marshes.
2. During the past 13,400 years, three abrupt centennial vegetation shift events occurred in the lake catchment around 12,300, 6500, and 300 cal. a BP when regional vegetation composition changed significantly, suggesting possible centennial-scale abnormal climatic and human-induced events.
3. Regional vegetation dynamics in the Lake YZH catchment were associated with hydrothermal conditions during the lateglacial and early–mid Holocene, and with human activities mainly during the late Holocene, especially after about 800 cal. a BP.
4. As a large lake, the pollen source of Lake YZH is complex. Although plant abundances estimated from the REVEALS model provided useful help in regional vegetation interpretation of fossil pollen records, certain uncertainties were still not negligible in estimated plant abundances of regional vegetation composition.

Author Contributions: Conceptualization, C.S. and M.W.; methodology, M.W., Q.S., H.M., H.Z. and C.S.; software, M.W. and Q.S.; validation, Q.S., H.M., L.H. and C.S.; formal analysis, M.W. and Q.S.; investigation, Q.S., H.M., L.H., H.L. and H.Z.; resources, L.H., H.L. and H.Z.; data curation, H.M. and C.S.; writing—original draft preparation, M.W.; writing—review and editing, C.S.; visualization, M.W.; supervision, C.S. and H.Z.; project administration, C.S.; funding acquisition, C.S., H.M., M.W. and H.L. All authors have read and agreed to the published version of the manuscript.

Funding: This research was funded by the National Natural Science Foundation of China: 42177437, 42167065, 41807447, 41601201, 41372191; Special Project for Basic Research of Yunnan Province—Key Project: 202101AS070006; Youth talent support program of Xingdian Talent Plan Yunnan Provence: XDYC-QNRC-2022-0029; the Yunnan Project for the Introduction of Advanced Talents: 2013HA024; Yunnan Normal University Postdoctoral Research Project; Yunnan Normal University Faculty of Geography Postdoctoral Fund: YNNU-FG-201; Yunnan Normal University Faculty of Geography Open Fund: YNNU-FG-202.

Data Availability Statement: The datasets used and generated in this study are available from the corresponding author on a reasonable request.

Conflicts of Interest: The authors declare no conflict of interest.

References

1. van der Maarel, E.; Franklin, J. *Vegetation Ecology*; Wiley-Blackwell: Chichester, UK, 2012.
2. Intergovernmental Panel on Climate Change (IPCC). *Climate Change 2021: The Physical Science Basis*; Cambridge University Press: Cambridge, UK, 2021.
3. Strandberg, G.; Lindström, J.; Poska, A.; Zhang, Q.; Fyfe, F.; Githumbi, E.; Kjellstrm, E.; Mazier, F.; Nielsen, A.B.; Sugita, S.; et al. Mid-Holocene European climate revisited: New high-resolution regional climate model simulations using pollen-based land-cover. *Quat. Sci. Rev.* **2022**, *281*, 107431. [CrossRef]
4. Tang, L.; Shen, C.; Lu, H.; Li, C.; Ma, Q. Fifty years of Quaternary palynology in the Tibetan Plateau. *Sci. China Earth Sci.* **2021**, *64*, 1825–1843. [CrossRef]
5. Shen, J.; Xue, B.; Wu, J.; Wu, Y.; Liu, X.; Yang, X.; Liu, J.; Wang, S. *Lake Sedimentation and Environmental Evolution*; Science Press: Beijing, China, 2010. (In Chinese)
6. Birks, H.J.B.; Birks, H.H. *Quaternary Palaeoecology*; Edward Arnold: London, UK, 1980.
7. Smol, J.P.; Birks, H.J.B.; Last, W.M. (Eds.) *Tracking Environmental Change Using Lake Sediments: Terrestrial, Algal, and Siliceous Indicators*; Kluwer Academic Publishers: New York, NY, USA, 2001; Volume 3.
8. Wang, S. *The Holocene Climate Change*; China Meteorological Press: Beijing, China, 2011. (In Chinese)
9. Li, B.; Zhang, W.; Fyfe, R.; Fan, B.; Wang, S.; Xu, Q.; Zhang, N.; Ding, G.; Yang, J.; Li, Y. High-resolution quantitative vegetation reconstruction in the North China Plain during the early-to-middle Holocene using the REVEALS model. *Catena* **2024**, *234*, 107577. [CrossRef]
10. Alley, R.B.; Meese, D.A.; Shuman, C.A.; Gow, A.J.; Taylor, K.C.; Grootes, P.M.; Whitell, J.W.C.; Ram, M.; Waddingto, E.D.; Mayewski, P.A.; et al. Abrupt increase in Greenland snow accumulation at the end of the Younger Dryas event. *Nature* **1993**, *362*, 527–529. [CrossRef]
11. Rasmussen, S.O.; Bigler, M.; Blockley, S.P.; Blunier, T.; Buchardt, S.L.; Clausen, H.B.; Cvijanovic, I.; Dahl-Jensen, D.; Johnsen, S.J.; Fischer, H.; et al. A stratigraphic framework for abrupt climatic changes during the last glacial period based on three synchronized Greenland ice-core records: Refining and extending the INTIMATE event stratigraphy. *Quat. Sci. Rev.* **2014**, *106*, 14–28. [CrossRef]
12. Dansgaard, W. Ice core evidence of abrupt climatic changes. In *Abrupt Climatic Change: Evidence and Implications*; Berger, W.H., Labeyria, D.L., Eds.; D. Reidel Publishing Company: New York, NY, USA, 1987; pp. 223–233.
13. Alley, R.B.; Mayewski, P.; Sowers, T.; Stuiver, M.; Taylor, K.C.; Clark, P.U. Holocene climatic instability: A prominent, widespread event 8200 yr ago. *Geology* **1997**, *25*, 486–583. [CrossRef]
14. Wu, W.; Liu, T. Possible role of the "Holocene event 3" on the collapse of Neolithic cultures around the central plain of China. *Quat. Int.* **2004**, *117*, 153–166.
15. Wang, B.; LinHo. Rainy Season of the Asian-Pacific Summer Monsoon. *J. Clim.* **2002**, *15*, 386–398. [CrossRef]
16. Chen, F.; Chen, X.; Chen, J.; Zhou, A.; Wu, D.; Tang, L.; Zhang, X.; Huang, X.; Yu, J. Holocene vegetation history, precipitation changes and Indian Summer Monsoon evolution documented from sediments of Xingyun Lake, southwest China. *J. Quat. Sci.* **2014**, *29*, 661–674. [CrossRef]
17. Xiao, X.; Haberle, S.G.; Li, Y.; Liu, E.; Shen, J.; Zhang, E.; Yin, J.; Wang, S. Evidence of Holocene climatic change and human impact in northwestern Yunnan Province: High-resolution pollen and charcoal records from Chenghai Lake, southwestern China. *Holocene* **2017**, *28*, 127–139. [CrossRef]
18. Jiang, W.; Leroy, S.A.G.; Yang, S.; Zhang, E.; Wang, L.; Yang, X.; Rioual, P. Synchronous strengthening of the Indian and East Asian Monsoons in response to global warming since the last Deglaciation. *Geophys. Res. Lett.* **2019**, *46*, 3944–3952. [CrossRef]
19. Zhang, X.; Zheng, Z.; Huang, K.; Yang, X.; Tian, L. Sensitivity of altitudinal vegetation in southwest China to changes in the Indian summer monsoon during the past 68000 years. *Quat. Sci. Rev.* **2020**, *239*, 106359. [CrossRef]
20. Xu, Y.; Guo, Q.; Yan, H. *A Study on the Impact of Climate Change on Forests in China*; Popular Science Press: Beijing, China, 1997. (In Chinese)
21. Wang, M.; Meng, H.; Huang, L.; Sun, Q.; Zhang, H.; Shen, C. Vegetation succession and forest fires over the past 13 000 years in the catchment of Yangzonghai Lake, Yunnan. *Quat. Sci.* **2020**, *40*, 175–189. (In Chinese)
22. Wang, S.; Du, H. *Annals of Lakes in China*; Science Press: Beijing, China, 1998. (In Chinese)
23. Yang, L.; Li, H. (Eds.) *Wetlands of Yunnan*; China Forestry Publishing House: Beijing, China, 2010. (In Chinese)
24. Wu, Z.; Zhu, Y.; Jiang, H. (Eds.) *Vegetation of Yunnan*; Science Press: Beijing, China, 1987. (In Chinese)
25. Zhu, Y. Study on environment background of Yangzonghai Lake basin. *Environ. Sci. Surv.* **2008**, *27*, 75–78. (In Chinese)
26. Faegri, K.; Iversen, J. *Textbook of Pollen Analysis*; Macmillan: New York, NY, USA, 1975.
27. Stockmar, J. Tablets with spores used in absolute pollen analysis. *Pollen Spores* **1971**, *13*, 615–621.
28. Grimm, E.C. TILIA and TILIA.GRAPH: PC spreadsheet and graphics software for pollen data. (Version 2.0.b.4.). *INQUA Comm. Study Holocene Work.-Group Data Handl. Methods Newsl.* **1990**, *4*, 5–7.

29. Grimm, E.C. CONISS: A FORTRAN 77 program for stratigraphically constrained cluster analysis by the method of incremental sum of squares. *Comput. Geosci.* **1987**, *13*, 13–35. [CrossRef]
30. Jacobson, G.L., Jr.; Grimm, E.C. A numerical analysis of Holocene forest and prairie vegetation in central Minnesota. *Ecology* **1986**, *67*, 958–966. [CrossRef]
31. Theuerkauf, M.; Couwenberg, J.; Kuparinen, A.; Liebscher, V. A matter of dispersal: REVEALSinR introduces state-of-the art dispersal models to quantitative vegetation reconstruction. *Veg. Hist. Archaeobotany* **2016**, *25*, 541–553. [CrossRef]
32. R Core Team. *R: A Language and Environment for Statistical Computing*; R Foundation for Statistical Computing: Vienna, Austria, 2023; Available online: https://www.R-project.org/ (accessed on 26 December 2023).
33. Hellman, S.; Gaillard, M.; Broström, A.; Sugita, S. The REVEALS model, a new tool to estimate past regional plant abundance from pollen data in large lakes: Validation in southern Sweden. *J. Quat. Sci.* **2008**, *23*, 21–42. [CrossRef]
34. Wan, Q.; Huang, K.; Chen, C.; Tang, Y.; Zhang, X.; Zhang, Z.; Zheng, Z. Relative pollen productivity estimates for major plant taxa in middle subtropical China. *Land* **2023**, *12*, 1337. [CrossRef]
35. Chen, H.; Xu, Q.; Zhang, S.; Sun, Y.; Wang, M.; Zhou, Z. Relative pollen productivity estimates of subtropical evergreen and deciduous broadleaved mixed forest in Ta-pieh Mountains. *Quat. Sci.* **2019**, *39*, 469–482. (In Chinese)
36. Zhang, Y.; Marquer, L.; Cui, Q.; Zheng, Z.; Zhao, Y.; Wan, Q.; Zhou, A. Holocene vegetation changes in the transition zone between subtropical and temperate ecosystems in Eastern Central China. *Quat. Sci. Rev.* **2021**, *253*, 106768. [CrossRef]
37. Wieczorek, M.; Herzschuh, U. Compilation of relative pollen productivity (RPP) estimates and taxonomically harmonised RPP datasets for single continents and Northern Hemisphere extratropics. *Earth Syst. Sci. Data* **2020**, *12*, 3515–3528. [CrossRef]
38. Wan, Q.C.; Zhang, Y.Z.; Huang, K.Y.; Sun, Q.W.; Zhang, X.; Gaillard, M.J.; Xu, Q.H.; Li, F.R.; Zheng, Z. Evaluating quantitative pollen representation of vegetation in the tropics: A case study on the Hainan Island, tropical China. *Ecol. Indic.* **2020**, *114*, 106297. [CrossRef]
39. Blaauw, M. Methods and code for 'classical' age-modelling of radiocarbon sequences. *Quat. Geochronol.* **2010**, *5*, 512–518. [CrossRef]
40. Reimer, P.J.; Austin, W.E.; Bard, E.; Bayliss, A.; Blackwell, P.G.; Ramsey, C.B.; Butzin, M.; Cheng, H.; Edwards, R.L.; Friedrich, M.; et al. The IntCal20 northern hemisphere radiocarbon age calibration curve (0-55 cal ka BP). *Radiocarbon* **2020**, *62*, 725–757. [CrossRef]
41. Sugita, S. Theory of quantitative reconstruction of vegetation I: Pollen from Large Sites REVEALS regional vegetation composition. *Holocene* **2007**, *17*, 229–241. [CrossRef]
42. Sugita, S.; Parshall, T.; Calcote, R.; Walker, K. Testing the landscape reconstruction algorithm for spatially explicit reconstruction of vegetation in northern Michigan and Wisconsin. *Quat. Res.* **2010**, *74*, 289–300. [CrossRef]
43. Serge, M.A.; Mazier, F.; Fyfe, R.; Gaillard, M.-J.; Klein, T.; Lagnoux, A.; Galop, D.; Githumbi, E.; Mindrescu, M.; Nielsen, A.B.; et al. Testing the effect of relative pollen productivity on the REVEALS model: A validated reconstruction of Europe-wide Holocene vegetation. *Land* **2023**, *12*, 986. [CrossRef]
44. Briks, H.J.B.; Gordon, A.D. *Numerical Methods in Quaternary Pollen Analysis*; Academic Press: London, UK, 1985.
45. Yunnan Forest Writing Committee. *Forests of Yunnan*; Yunnan Science and Technology Press & China Forestry Publishing House: Kunming, China, 1986. (In Chinese)
46. Matthias, I.; Giesecke, T. Insights into pollen source area, transport and deposition from modern pollen accumulation rates in lake sediments. *Quat. Sci. Rev.* **2014**, *87*, 12–23. [CrossRef]
47. Xiao, X.; Yao, A.; Hillman, A.; Shen, J.; Haberle, S.G. Vegetation, climate and human impact since 20 ka in central Yunnan Province based on high-resolution pollen and charcoal records from Dianchi, southwestern China. *Quat. Sci. Rev.* **2020**, *236*, 106279. [CrossRef]
48. Sun, Q. Spatio-Temporal Changes of Vegetation, Climate, and Forest Fire Since the Last Glacial Maximum and Their Driving Mechanisms in Typical Lake Basins of Yunnan. Ph.D. Thesis, Yunnan Normal University, Kunming, China, 2023. (In Chinese).
49. Chen, X.; Wu, D.; Huang, X.; Lv, F.; Brenner, M.; Jin, H.; Chen, F. Vegetation response in subtropical southwest China to rapid climate change during the Younger Dryas. *Earth-Sci. Rev.* **2020**, *201*, 103080. [CrossRef]
50. Wu, J.; Shen, C.; Yang, H.; Shi, Q.; Xie, S.C. Holocene temperature variability in China. *Quat. Sci. Rev.* **2023**, *312*, 107184. [CrossRef]
51. Wang, Y.; Cheng, H.; Edwards, R.L.; He, Y.; Kong, X.; An, Z.; Wu, J.; Kelly, M.J.; Dykoski, C.A.; Li, X. The Holocene Asian monsoon: Links to solar changes and North Atlantic climate. *Science* **2005**, *308*, 854–857. [CrossRef] [PubMed]
52. Dykoski, C.A.; Edwards, R.L.; Cheng, H.; Yuan, D.; Cai, Y.; Zhang, M.; Lin, Y.; Qing, J.; An, Z.; Revenaugh, J. A high-resolution, absolute-dated Holocene and deglacial Asian monsoon record from Dongge Cave, China. *Earth Planet. Sci. Lett.* **2005**, *233*, 71–86. [CrossRef]
53. Zou, Q.; Miao, W. *Chinese Population (Yunnan Province)*; China Financial and Economic Publishing House: Beijing, China, 1989. (In Chinese)
54. Shi, Q.; Shen, C.; Meng, H.; Huang, L.; Sun, Q. A 1640-Year vegetation and fire history of the Lake Haixihai catchment in northwestern Yunnan, Southwest China. *Forests* **2023**, *14*, 990. [CrossRef]
55. Chen, F.; Zhang, J.; Liu, J.; Cao, X.; Hou, J.; Zhu, L.; Xu, X.; Liu, X.; Wang, M.; Wu, D.; et al. Climate change, vegetation history, and landscape responses on the Tibetan Plateau during the Holocene: A comprehensive review. *Quat. Sci. Rev.* **2020**, *243*, 106444. [CrossRef]
56. Li, X.; Walker, D. The plant geography of Yunnan Province, southwest China. *J. Biogeogr.* **1986**, *13*, 367–397.

57. Fu, L.-G. A study of *Ulmus* in China. *J. Northeast. Forest. Inst.* **1980**, *3*, 3–42. (In Chinese)
58. Shen, J.; Xiao, X. Evolution of the South Asian monsoon during the last 20 ka recorded in lacustrine sediments from Southwestern China. *Quat. Sci.* **2018**, *38*, 799–820. (In Chinese)
59. Shen, C. Millennial-Scale Variations and Centennial-Scale Events in the Southwest Aian Monsoon: Pollen Evidence from Tibet. Ph.D. Thesis, Louisiana State University, Baton Rouge, LA, USA, 2003.
60. Bond, G.; Broecker, W.; Johnsen, S.; McManus, J.; Labeyrie, L.; Jouzel, J.; Bonani, G. Correlations between climate records from North Atlantic sediments and Greenland ice. *Nature* **1993**, *365*, 143–147. [CrossRef]
61. Hicks, S.; Hyvärinen, H. Pollen influx values measured in different sedimentary environments and their palaeoecological implications. *Grana* **1999**, *38*, 228–242. [CrossRef]
62. Dong, X.; Wu, Y. *Vicissitudes of Lake Dianchi: Millennium Environmental History Perspective*; Intellectual Property Publishing House: Beijing, China, 2013. (In Chinese)
63. Fitzgerald, C.D. *The Southern Expansion of the Chinese People*; Australian National University Press: Canberra, Australia, 1972.

Disclaimer/Publisher's Note: The statements, opinions and data contained in all publications are solely those of the individual author(s) and contributor(s) and not of MDPI and/or the editor(s). MDPI and/or the editor(s) disclaim responsibility for any injury to people or property resulting from any ideas, methods, instructions or products referred to in the content.